Indirect Photolysis of Organic Compounds: Prediction of OH Reaction Rate Constants through Molecular Orbital Calculations

Anna Böhnhardt,[†,‡] Ralph Kühne,[†] Ralf-Uwe Ebert,[†] and Gerrit Schüürmann*[,†,‡]

UFZ Department of Ecological Chemistry, Helmholtz Centre for Environmental Research, Permoserstrasse 15, 04318 Leipzig, Germany, and Institute for Organic Chemistry, Technical University Bergakademie Freiberg, Leipziger Strasse 29, 09596 Freiberg, Germany

Received: June 13, 2008; Revised Manuscript Received: July 31, 2008

The MOOH approach is a perturbational molecular orbital method to predict rate constants of indirect photolysis of organic compounds through reaction with OH radicals. It employs the semiempirical AM1 scheme as the underlying quantum chemical model. The original method introduced by Klamt has been reparametrized using an up-to-date set of 675 compounds with experimental rate constants and outperforms the prominent Atkinson increment scheme for this training set as well as for an extended set of 805 compounds, yielding an overall root-mean-square error of 0.32 log units. The discussion includes detailed comparative analyses of the model performances for individual compound classes. The present model calibration refers mainly to monofunctional compounds but performs already reasonably well for multifunctional compounds. For predictive applications, both the Atkinson scheme and the alternative, independent AM1-MOOH model can be used as components of a consensus modeling approach, arriving at increased confidence in cases where the different models agree.

Introduction

Reaction with OH radicals is the major tropospheric sink for most volatile organic compounds. Therefore, the respective rate constants largely determine the atmospheric residence time and are crucial for environmental fate modeling and risk assessment.

The measurement of rate constants of the indirect photolysis through reaction with OH radicals, k_{OH}, is expensive and time-consuming, calling for models to predict such constants directly from molecular structure. In particular, respective prediction methods would allow one to identify, at an early stage of environmental assessment, compounds that are likely to meet the conditions of persistent organic pollutants (POPs), and as such yield pertinent information in the context of REACH (registration, evaluation, and authorization of industrial chemicals; EC 1907/2006), the new European Community Regulation on industrial chemicals and their safe use. Moreover, methods to predict the atmospheric lifetime and long-range transport of chemical substances can be used as tool to support the design of environmentally benign compounds. Environmental risk assessment procedures that use estimation methods for screening are another field of application.

So far, Atkinson's increment scheme[1−3] is the only method generally used for predicting k_{OH}, requiring two-dimensional (2D) molecular structures as only input information. This increment method uses basic rate constants for specific reaction sites and quantifies the influence of neighboring groups through fixed group factors, relying on the additivity of intramolecular effects as major assumption inherent to all respective increment schemes.

Some time ago, Klamt had introduced an independent approach, the MOOH (molecular orbital OH) method.[4,5] This method calculates local electronic properties of 3D molecular structures, employing semiempirical quantum chemistry. More specifically, it employs local molecular parameters and thus accounts also for nonlinear intramolecular interactions as far as these are captured in the level of quantum chemical calculation chosen. Despite the fact that this method is based on a fundamental approach and employs much less parameters than the Atkinson scheme, its use has been limited so far,[6−8] and there is little knowledge about its performance for larger data sets.

In the present study, the statistical performances of the MOOH method and the Atkinson method were evaluated using a large set of organic compounds with up-to-date experimental k_{OH} values, and the MOOH method was recalibrated using the current data set. The goal was to establish the MOOH approach as working alternative to the Atkinson method, thus offering two independent ways to predict k_{OH} from molecular structure. In this way, confidence in predicted k_{OH} values can be enhanced through comparison of the results from these two methods that rely on quite different methodological assumptions and calculation procedures.

Materials and Methods

Data Set. Experimental values for the second-order rate constant of indirect photolysis through reaction with OH radicals, k_{OH}, have been collected from literature and subjected to critical analysis. The compound set was selected such that it belongs to the mechanistic domain of the MOOH method, the latter of which is defined as follows: Abstraction of hydrogen atoms from sp^3 carbon atoms ($k^{C}_{H\text{-}abs}$), H abstraction from aliphatic carbon enhanced through lone pairs of neighbor oxygen ($k^{C(O)}_{H\text{-}abs}$), abstraction of aldehydic H ($k^{CHO}_{H\text{-}abs}$), OH addition to aromatic atoms (k^{aro}_{add}), OH addition to double and triple bonds ($k^{C=C}_{add}$, $k^{C\equiv C}_{add}$), and H abstraction from the hydroxyl groups of alcohols and carboxylic acids ($k^{OH}_{H\text{-}abs}$). The mechanistic domain

* Corresponding author. Tel:+49-341-235-1262. Fax: +49-341-235-1785. E-mail: gerrit.schuurmann@ufz.de.
† UFZ Helmholtz Centre for Environmental Research.
‡ Technical University Bergakademie Freiberg.

10.1021/jp8052218 CCC: $40.75
Published on Web 10/17/2008

is thus defined through compounds where the overall k_{OH} may cover the following individual contributions:

$$k_{OH} = \sum k_{H\text{-}abs}^{C} + \sum k_{H\text{-}abs}^{C(O)} + \sum k_{H\text{-}abs}^{CHO} + \sum k_{add}^{aro} + \sum k_{add}^{C=C} + \sum k_{add}^{C\equiv C} + \sum k_{H\text{-}abs}^{OH} \quad (1)$$

For a given molecule, each intramolecular reaction site with its site-specific reaction mechanism needs to be taken into account, yielding the second-order rate constant k_{OH} as sum of all individual rate constants. Because k_{OH} covers several orders of magnitude and ranges from 1.91×10^{-16} (pentafluoromethyl ether) to 5.5×10^{-10} (1-naphthol) cm^3 $molecule^{-1}$ s^{-1}, log k_{OH} is the target property for model calibration and prediction. A table with the 805 experimental k_{OH} data used for the present study is given as Supporting Information.

Software. The program AOPWIN[9,10] was used to perform the calculations according to the Atkinson method. Semiempirical AM1[11] calculations have been carried out with the MOPAC package.[12] These calculations usually require only some seconds time per molecule (including geometry optimization) and may be conducted quickly for a large number of compounds. The original MOOH FORTRAN subroutine was modified and included in a separate FORTRAN program that imports the required information from the respective MOPAC output files and from our in-house software ChemProp.[13] In addition, unrestricted density functional theory calculations employing B3LYP/6-31++G**[14−19] were carried out with the GAUSSIAN 03 package.[20]

MOOH Calibration. For the total set of 805 compounds, geometry optimizations were carried out at the AM1[11] level. The resultant MOPAC output files were used as molecule-specific input files for all of the following MOOH calculations. The MOOH method contains nonlinear model equations that were initially calibrated using 260 compounds.[4,5] For its recalibration, the Marquardt method[21] was implemented on the basis of a FORTRAN algorithm from literature.[22] Because H abstraction from saturated carbon (sp^3 hybridization) is usually much slower than the other reaction mechanisms involving the OH radical, the following calibration strategy was employed: First, the subset of 233 saturated hydrocarbons and ethers was used to fit the model equation for H abstraction. Then, the other reaction mechanisms were calibrated separately, using subsets of compounds that offered only H abstraction from sp^3 carbon and the respective additional mechanism. In this way, we avoided the possibility of contaminating the model equation for one fast reaction mechanism through the presence of a second fast reaction pathway, assuming that the overall degradation rate can be decomposed into individual reaction-specific degradation rates according to eq 1. For the same line of reasoning, multifunctional compounds offering more than one degradation pathway with similar degradation kinetics were excluded from calibration to avoid cross-contamination of pathway-specific parameters. Thus, only 675 compounds of the total set of 805 compounds were used for calibration (training set). Details of the reaction-specific subset selections are given below together with the recalibrated MOOH model equations (see Results and Discussion).

Statistical Performance. The calibration performance was quantified through the squared correlation coefficient r^2. In addition, the predictive squared correlation coefficient,

$$q^2 = 1 - \frac{\sum_i (y_i^{pred} - y_i^{obs})^2}{\sum_i (y_i^{obs} - y^{mean})^2} \quad (2)$$

was used to assess the prediction performance. In eq 2, y_i^{pred} and y_i^{obs} denote the predicted (not fitted) and observed target value of compound i (in our case: log k_{OH}), and y_i^{mean} the experimental mean value of the data set. Note that r^2 can be defined through eq 2 with y_i^{pred} being replaced by y_i^{fit}, the regression-fitted target value. It automatically corrects for systematic errors also if applied to existing regression models, has a value range between 0 (no correlation) and 1 (perfect correlation), and focuses on the trend rather than on absolute values. By contrast, q^2 ranges from 1 (perfect agreement) to $-\infty$, with $q^2 = 0$ representing the case where the model prediction is as good as taking the experimental mean as predictor for all values (cf. ref 23). When a regression model is derived, $q^2 = r^2$ for the training set in the case of parallel calibration of all multilinear parameters (because in this case $y_i^{pred} = y_i^{fit}$). In our case, however, $q^2 \leq r^2$ for the total compound set because of two reasons: First, only 675 of the 805 compounds were used as the AM1-MOOH training set, and second, we employed a stepwise parameter calibration as indicated above (and specified below when presenting the results). Generally, the closer q^2 is to r^2 when applying the model to compounds outside the training set, the better is its prediction capability.

In addition, the following parameters have been used to further characterize the statistical performance: root-mean-square error (*rms*), systematic error (*bias*), mean error (*me*), maximum negative error (*mne*, largest underestimation), and maximum positive error (*mpe*, largest overestimation).

Reaction Mechanisms of Indirect Photolysis

For most organic compounds, the initial step of atmospheric oxidation proceeds by reaction with OH radicals. Depending on the chemical structure of the respective compound, the OH attack may occur via several mechanisms:

Aliphatic compounds are degraded by hydrogen abstraction reactions from sp^3 carbons.[24,25] Usually, these reactions are rather slow as compared to other OH reaction mechanisms. Their importance results from the abundant occurrence of respective reaction sites in most organic compounds:

$$CH_4 + HO^{\bullet} \xrightarrow{k_{H\text{-}abs}^{C}} CH_3^{\bullet} + H_2O \quad (3)$$

Abstraction may take place directly (see eq 3), or in the case of hydrogen bond acceptors, via prereactive complexes:[26−34]

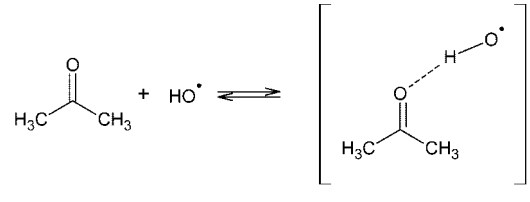

(4)

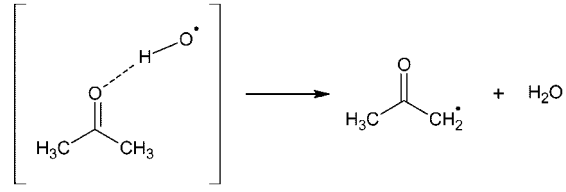

(5)

This latter mechanism enhances the overall hydrogen abstraction rate from aliphatic carbons:

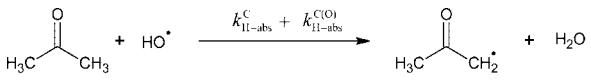

(6)

Abstraction of hydrogen atoms from hydroxyl or carboxyl groups is another possible OH radical reaction pathway of oxygenated organic compounds (see the last term in eq 1 that sums over all respective sites with associated rate constants $k^{OH}_{H\text{-abs}}$).

Aldehydes mainly react by hydrogen abstraction from the CHO group:[24,25]

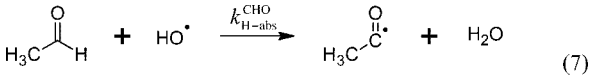

(7)

Furthermore, hydrogen abstraction from alkyl side chains (with carbonyl oxygen serving as hydrogen bond acceptor) is possible.

For unsaturated compounds, addition to multiple bonds is the major reaction pathway. OH radicals may add to aromatic rings as well as to double and triple bonds:[24,25]

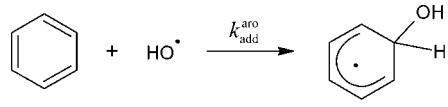

(8)

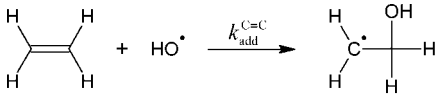

(9)

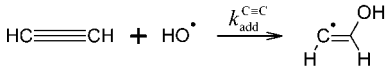

(10)

Again, hydrogen abstraction from alkyl side chains may be an additional but minor degradation pathway for these compounds.

Site-Specific Reactivity by Local Molecular Parameters

Background and Notation. Local molecular parameters are derived from semiempirical or ab initio quantum chemical calculations, and contain information about the electronic status of the respective reaction site. The underlying framework is given by the linear combination of atomic orbitals (LCAO) to give molecular orbitals (MO), the LCAO-MO approach. In contrast to conventional MO-based parameters[35] such as the frontier orbital energies HOMO and LUMO (highest occupied and lowest unoccupied molecular orbital), the parameters described in more detail below have been designed to extract, from the delocalized MO wave functions and energies, energy and charge information that reflects the local characteristics of a given atomic site in the molecular environment.

In the following outline, latin indices i, j refer to molecular orbitals occupied in the electronic ground state, k and l denote unoccupied molecular orbitals, greek indices μ and μ specify atomic orbitals (AO), and r and s denote atomic sites within a given molecule. The contribution of the μth AO to the ith MO is given by the LCAO-MO coefficient $c_{\mu i}$. The notation $\mu(r)$ indicates that only AOs μ located at atomic site r are taken into account. The energy of the ith MO is represented by E_i.

Charge-Limited Donor Energy. The electronic parameter important for hydrogen abstraction from aliphatic and aldehydic carbon (eqs 3 and 7) as well as for the addition to double and triple bonds (eqs 9 and 10) is the energy required to donate charge q from atomic site r:

$$EQ_{occ}(q,r) = \sum_{i=\mathrm{HOMO}}^{1} E_i \cdot w_q(i,r)$$

$$w_q(i,r) = \begin{cases} 2q^{-1}\sum_{\mu(r)} c_{\mu i}^{\,2} & \text{if } 2\sum_{j=\mathrm{HOMO}}^{i}\sum_{\mu(r)} c_{\mu j}^{\,2} < q \\ 1 - 2q^{-1}\sum_{m=\mathrm{HOMO}}^{i+1}\sum_{\mu(r)} c_{\mu m}^{\,2} & \text{if } 2\sum_{m=\mathrm{HOMO}}^{i+1}\sum_{\mu(r)} c_{\mu m}^{\,2} \le q \le 2\sum_{j=\mathrm{HOMO}}^{i+1}\sum_{\mu(r)} c_{\mu j}^{\,2} \\ 0 & \text{if } 2\sum_{m=\mathrm{HOMO}}^{i+1}\sum_{\mu(r)} c_{\mu m}^{\,2} > q \end{cases} \quad (11)$$

This local charge-limited donor energy is calculated as weighted mean of the topmost doubly occupied molecular orbital energies. Starting with the HOMO, the energies of occupied MOs i contributing $c_{\mu i}^2$ electron charge to atomic site r through AOs $\mu(r)$ are taken into account until the predefined charge limit (cutoff) q is reached.

Effective Donor Energy. Starting from the HOMO, an effective donor energy at atomic site r, $EE_{occ}(r)$, is calculated as weighted mean of all doubly occupied MOs, considering both their individual energies E_i and their charge contributions $c_{\mu i}^2$ that result from the LCAO-MO coefficients of AOs $\mu(r)$. The exponential energy term of the weight factor contains a predefined reference energy E_{ref} to normalize E_i in a suitable way:

$$EE_{occ}(E_{ref},r) = \sum_{i=\mathrm{HOMO}}^{1} E_i \cdot w_{ref}(i,r)$$

$$w_{ref}(i,r) = \frac{\sum_{\mu(r)} c_{\mu i}^{\,2} \cdot \exp\left\{\frac{E_i}{E_{ref}}\right\}}{\sum_{j=\mathrm{HOMO}}^{1}\left(\sum_{\nu(r)} c_{\nu j}^{\,2} \cdot \exp\left\{\frac{E_j}{E_{ref}}\right\}\right)} \quad (12)$$

In this way, both the energy and the extent of the local character of the electron charge are taken into account. This parameter has turned out to provide pertinent information about the site-specific reactivity of aromatic carbon toward OH addition (eq 8).

Energy-Limited Acceptor Charge. This parameter quantifies the energy associated with accepting additional charge at atomic site r. It contributes to the site-specific reactivity for OH addition at double bonds (eq 9). Starting with the LUMO, the unoccupied MOs k with energies E_k are considered, using the squared LCAO-MO coefficients $c_{\mu k}^2$ as measure for the acceptor capacity of r. The latter is limited by a predefined penetration energy ε.

TABLE 1: Deformation Energies Δ^{aro}_{def} Relative to Hydrogen (in kcal/mol)[4]

atom type	−S−	−H	−I	−Br	−C_{any}	−Cl	−O−	−NO_2	−F	−N <
Δ^{aro}_{def}	−3	0	0	3	5	6	8	8	11	19

In this way, $QE_{vac}(\varepsilon,r)$ characterizes the charge acceptor capacity of atomic site r that is available up to the penetration energy ϵ:

$$QE_{vac}(\varepsilon,r) = 2 \cdot \sum_{k=\mathrm{LUMO}}^{n} \sum_{\mu(r)} {c_{\mu k}}^2 \cdot w_k(\varepsilon)$$

$$w_k(\varepsilon) = \begin{cases} 1 & \text{if } E_k < \varepsilon - 0.5 \\ (E_k - \varepsilon) + 0.5 & \text{if } \varepsilon - 0.5 \le E_k \le \varepsilon + 0.5 \\ 0 & \text{if } E_k > \varepsilon + 0.5 \end{cases} \quad (13)$$

Systems with π Electrons. Atomic π orbitals are of major interest for the characterization of π systems like alkenes. To account for this aspect, the local molecular parameters may be calculated for the respective π orbitals alone instead of summing over all atomic orbitals. In the following, the index π denotes these π-specific parameters in the respective formula.

Deformation Energy. Addition to aromatic rings is expected to occur preferably at unsubstituted carbon atoms (see eq 8). To account for the additional energy demand in the case of substituted aromatic carbon, Klamt[4] introduced a deformation energy Δ_{def}^{aro}, describing the energy required to bend the substituent of the respective aromatic carbon by 45° from planarity. AM1 calculations showed that Δ_{def}^{aro} is principally determined by the atom type of the first substituent atom.[4] Accordingly, a list of Δ_{def}^{aro} values for the most common substituent atom types (see Table 1) has been generated[4] for both calibration and prediction purposes. Δ_{def}^{aro} has been set to 100 kcal/mol for the inner atoms of condensed aromatics,[4] as addition to these atoms is very unlikely.

Results and Discussion

In the regression equations presented below, the units are as follows: 10^{-12} cm^3 molecule^{-1} s^{-1} for rate constants, eV for MO energies, and electron charges e for charges.

Overall Statistics. As can be seen from Table 1, the recalibrated MOOH method ($q^2 = 0.94$, $rms = 0.32$) is slightly superior to its original Klamt parametrization ($q^2 = 0.93$, rms = 0.35) and to the Atkinson increment method ($q^2 = 0.92$, rms = 0.35) when using all 805 compounds. The only marginal improvement over the original MOOH model version that was based on 260 training set compounds demonstrates the robustness and sound basis of this quantum chemical approach to predict log k_{OH}. Nevertheless, the MOOH recalibration led to a significant improvement for individual compound classes as outlined below.

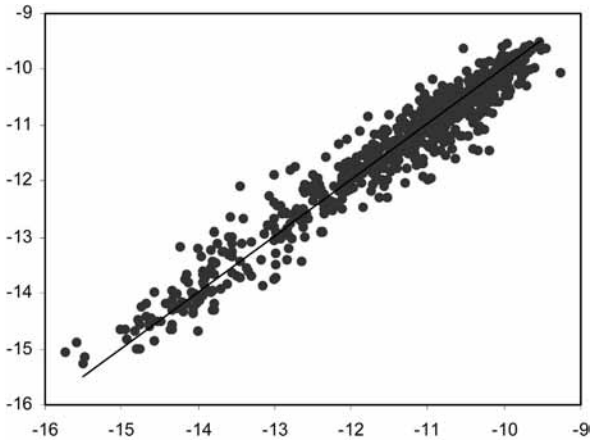

Figure 1. Calculated vs experimental log k_{OH} for the total data set of 805 compounds.

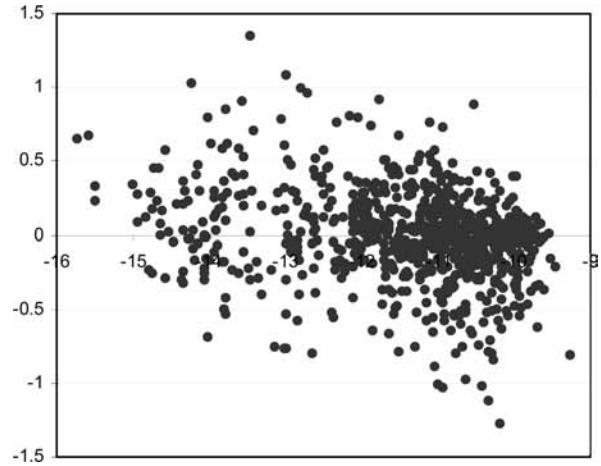

Figure 2. Calculation error vs experimental log k_{OH} for the total data set of 805 compounds.

With respect to individual outliers, MOOH outperforms the additive increment scheme (mne −1.3 vs −2.6 log units, mpe 1.3 vs 2.2 log units); the numbers of compounds exceeding 1 order of magnitude as error are 8 (AM1-MOOH), 15 (Klamt parametrization), and 24 (Atkinson). Remarkably, almost all (22 out of 24) these outliers of the Atkinson method are fluorinated compounds, a finding that is consistent with previous studies reporting larger deviations for halogenated compounds.[6] With AM1-MOOH, there are 6.2% (50 compounds) exceeding 2 *rms* (0.64 log units), and the respective numbers of outliers are 7.2% (58 compounds) for the original Klamt parametrization ($2 \cdot rms = 0.70$), and 6.5% (52 compounds) for the Atkinson increment method ($2 \cdot rms = 0.70$).

Overall, *rms* values of around 0.35 log units can be considered acceptable for screening purposes and for priority setting in the context of REACH, as well as for exploring the atmospheric lifetime of candidate structures when designing novel industrial chemicals. In this context, however, it is important to make sure that a given prediction model is applied only when the compound or molecular structure of interest belongs to the proper mechanistic domain (see eq 1 and "Reaction Mechanisms of Indirect Photolysis" with eqs 3−10 above).

In Figure 1, the data distribution of predicted vs experimental log k_{OH} is shown for the recalibrated MOOH method. Figure 2 shows the associated error distribution in terms of prediction error vs experimental log k_{OH}.

The latter distribution reveals an interesting trend: Overestimations (positive prediction errors) of log k_{OH} are observed more frequently with smaller log k_{OH}, and underestimations (negative prediction errors) occur more often with larger values for log k_{OH}. Similar error patterns have been observed also for the original Klamt parametrization as well as for the Atkinson increment scheme. It follows that with the presently available prediction methods for the indirect photolysis of organic substances through reaction with OH radicals, there is a slight tendency to overestimate log k_{OH} for less reactive compounds, and to underestimate log k_{OH} for more reactive compounds. For future work on a further refinement of the model parametrization, attention should be paid to this finding.

To examine whether the observed error trend is specific to certain subsets of our data, we grouped the data set in compounds according to the percentage of the largest calculated mechanistic contribution to the overall rate constant ($k_{H\text{-}abs}^{C}$, $k_{H\text{-}abs}^{C(O)}$, $k_{H\text{-}abs}^{CHO}$, k_{add}^{aro}, $k_{add}^{C=C}$, $k_{add}^{C\equiv C}$, or $k_{H\text{-}abs}^{OH}$). It became apparent that most of the calculated rate constants (666, 83%) can be related

to a major contribution accounting for more than 75% of the overall rate constant. The remaining 139 rate constants (17%) result from several OH reaction mechanisms contributing significantly to the overall value.

The rate constants dominated by a single contribution range from 1.91×10^{-16} to 5.5×10^{-10} cm^3 molecule^{-1} s^{-1}, whereas the subset of 139 substances composed of several significant terms contains larger rate constants ranging from 1.01×10^{-13} to 2.31×10^{-10} cm^3 molecule^{-1} s^{-1}. This is not surprising as the lowest rate constants are generally observed for haloalkanes and haloethers with hydrogen abstraction from sp^3 carbons ($k^{C}_{H\text{-}abs}$) being the only degradation pathway. The above-described tendency in the occurrence of under- and overestimations is observed for both subsets.

Moreover, the error trend was analyzed with respect to the individual degradation mechanisms. To this end, the data set was also divided into subsets according to the reaction type giving the largest calculated contribution to the overall rate constant ($k^{C}_{H\text{-}abs}$, $k^{C(O)}_{H\text{-}abs}$, $k^{CHO}_{H\text{-}abs}$, k^{aro}_{add}, $k^{C=C}_{add}$, $k^{C\equiv C}_{add}$, or $k^{OH}_{H\text{-}abs}$). Generally, all subsets except for the six rate constants assigned to $k^{C\equiv C}_{add}$ show the above-mentioned trend in error distribution. However, the tendency to overestimate small and to underestimate large rate constants is particularly significant for $k^{CHO}_{H\text{-}abs}$ and $k^{OH}_{H\text{-}abs}$. For the eight rate constants assigned to the $k^{OH}_{H\text{-}abs}$ subset, this trend is consistent with the fact that the $k^{OH}_{H\text{-}abs}$ mechanism is modeled by constant factors.

Hydrogen Abstraction from Aliphatic Carbon. The abstraction of hydrogen atoms from aliphatic carbon atoms is slow compared with other reaction mechanisms such as the addition of OH radicals to unsaturated bonds.[24,25] Therefore, calibration of the respective model equation requires a fitting set of compounds with hydrogen abstraction being the only OH degradation pathway. Following previous studies,[5,26−34] we assume the reaction of ketones, esters, alcohols and carboxylic acids to be accelerated by the formation of initial hydroxyl-adducts with the hydrogen bond acceptor groups of the molecules. This additional lone pair-enhanced reactivity is accounted for separately (see below).

Starting with the MOOH equation introduced by Klamt,[4] an updated set of 233 saturated hydrocarbons and ethers was used for the nonlinear recalibration. As halomethanes are not described satisfactorily by local molecular orbitals,[4] they were left out of the original fit as well as out of the recalibration procedure. We used the charge-limited donor energy $EQ_{occ}(0.18,r_H)$ as a descriptor for the reactivity at atomic sites H, summing over all H atoms attached to aliphatic carbon of a given molecule to predict its rate constant $k^{C}_{H\text{-}abs}$ for indirect photolysis through reaction with OH radicals (see eq 3). Nonlinear regression led to the following equation for the respective rate constant referring to a given H site r_H:

$$k^{C}_{H\text{-}abs}(r_H) = \exp\left\{\frac{11.79}{(1+\exp\{-3.25\cdot(EQ_{occ}(0.18,r_H)+10.7)\})^{0.17}} - 9.46\right\} \quad (14)$$

Summing over all respective sites with H attached to aliphatic carbon leads to the first term of eq 1. Though the regression *rms* is significantly smaller than the one achieved with the Atkinson method (0.28 vs 0.39, see Table 1), the latter performs better for halomethanes (keeping in mind that small compounds tend to be simpler for increment schemes by virtue of their incremental approach). The reason for the poor performance with halomethanes is still unclear and may be subject to future investigations.

Enhanced Reactivity for H Abstraction from Aliphatic Carbon. Oxygen lone pairs enhance the reactivity for H abstraction from aliphatic carbon through OH radicals. This can be traced back to the formation of hydrogen-bonded OH-acceptor complexes prior to the reaction between OH and H (see eqs 4 and 5).[4,5,26−34] Following Klamt, the reactivity enhancement is modeled through introduction of a lone pair factor w_i^{lp} that characterizes the susceptibility of the oxygen lone pair to interact with OH, and a steric factor f_i^{steric} that accounts for the spatial availability of the H atom for the attacking OH as well as for the distance between oxygen and the reaction site H of interest. This approach led to the following equation describing the enhanced reactivity for hydrogen atom abstraction:

$$k^{C(O)}_{H\text{-}abs} = k_{H\text{-}abs} \cdot \sum_i w_i^{lp} \cdot f_i^{steric} \quad (15)$$

with the overall reaction rate for hydrogen abstraction from aliphatic carbons being the sum of the terms $k^{C}_{H\text{-}abs}$ and $k^{C(O)}_{H\text{-}abs}$ (see eq 6). For a given H site at aliphatic carbon, the summation is carried out over all relevant oxygen lone pairs, considering ketones, esters, alcohols and carboxylic acids. Summing over all respective H sites provides the second term in eq 1. The steric factor on the rhs of eq 15 is given by

$$f_i^{steric} = \exp\left[-\frac{(d_i^{lp} - d_{opt}^{lp})^2}{2t^2}\right] \quad (16)$$

where d_i^{lp} is the distance between H (attached at aliphatic carbon) and oxygen i carrying the lone pair, d_{opt}^{lp} is the respective optimal distance, and t denotes the tolerance in the distance that was set to 0.7 Å. In the original MOOH parametrization, AM1 calculations had been used to derive $d_{opt}^{lp} = 2.5$ Å from OH−oxygen adducts.[5] Because AM1 is less reliable for predicting H-bonding geometries, we decided to employ the density functional method UB3LYP/6-31++G**[14−19] for this purpose. In this way, optimized lone pair positions were determined from OH−oxygen complexes for molecules representing the different compound classes.

The lone pair factor w_i^{lp} differs for different oxygen types. In the original MOOH method, two factors were used to describe the different oxygen lone pairs in oxygenated organic compounds. The first value, $w^{lp}_{C=O}$, was derived from ketones and was also used for the carbonyl oxygen in aldehydes and carboxylic acids (see next section below). The second value, w^{lp}_{OOR}, referred to ester carbonyl oxygen that has a distinctly less enhancing effect on hydrogen atom reactivity. It was also used for the sp^3 oxygen in hydroxyl groups of alcohols. The sp^3 oxygen of ester functions as well as ether oxygen are not considered to enhance the reactivity for H abstraction. Finally, Klamt introduced constant contributions for the abstraction of hydroxylic hydrogen atoms in alcohols and acidic hydrogen atoms in carboxylic acids.

For the present recalibration, 148 oxygenated compounds were used that included also bi- and multifunctional structures, thus broadening the range of applicability of the resultant parameters. Among the esters, the formyl group HC(O)O− offers an additional site of H abstraction (the formyl H attached to carbonyl carbon) that must not be neglected,[27] but that differs mechanistically from the oxygen-enhanced H abstraction from sp^3 carbon. Accordingly, formyl esters were excluded from the

calibration set, and the reaction was treated as abstraction of an aldehydic hydrogen (see below), leading to moderate results.

Initial analyses showed that the performance with oxygenated compounds could be improved when treating the sp^2 carbonyl oxygen of esters and the sp^3 oxygen of alcohols separately, resulting in a third lone pair factor w^{lp}_{OH} for alcohols. The new lone pair factors to be used in eq 15 are

$$w^{lp}_{C=O} = 24.5$$

$$w^{lp}_{OOR} = 3.42$$

$$w^{lp}_{OH} = 4.51 \quad (17)$$

The new MOOH constants to account for the additional option of H abstraction from hydroxyl groups ($k^{alc}_{H\text{-}abs}$) as well as from carboxylic acids ($k^{acid}_{H\text{-}abs}$) are

$$k^{alc}_{H\text{-}abs} \approx 0.04$$

$$k^{acid}_{H\text{-}abs} \approx 0.26 \quad (18)$$

These constants are applied such that for a given alcohol or carboxylic acid, the overall k_{OH} is calculated through adding $k^{alc}_{H\text{-}abs}$ or $k^{acid}_{H\text{-}abs}$ (per OH or OOH functionality) to the initial result calculated according to eq 1.

As can be seen from Table 2, the new MOOH calibration is superior to the initial parametrization, but still inferior to the Atkinson method for the set of 148 oxygenated compounds (*rms* values of 0.37, 0.43, and 0.31, respectively). The latter finding was surprising and may partly reflect shortcomings of the semiempirical wave functions of the underlying AM1 scheme. It suggests respective attention when dealing with this compound group in future investigations. Note further that because the original MOOH parametrization for ketones was confined to monofunctional compounds, it still performs slightly better for this subclass of compounds. The slight deviation between r^2 and q^2 results from the fact that the term $k^{C}_{H\text{-}abs}$ was calculated according to eq 14, and thus the overall rate constant k_{OH} consists of a predicted and a fitted part.

Aldehydic Reactivity. In the majority of cases, abstraction of aldehydic hydrogen is the dominating reaction pathway for aldehydes.[24,25,27] Because this hydrogen abstraction does not take place at aliphatic carbon atoms, but at sp^2 carbons (see eq 7), a new equation is required to describe the respective reactivity.

In addition, hydrogen abstraction from sp^3 carbon contributes to the overall k_{OH} for aldehydes, and here the above-described reactivity enhancement through oxygen lone pairs has to be taken into account. Following the original MOOH approach, we use the ketone lone pair factor $w^{lp}_{C=O}$ also for aldehydes, employing the value derived from UB3LYP/6-31++G** calculations as mentioned above. Taking into account H abstraction from both the aldehydic sp^2 carbon and from aliphatic sp^3 carbon, nonlinear regression led to the following equation for the former pathway:

$$k^{CHO}_{H\text{-}abs}(r_H) = 10^{\{1.53 \cdot EQ_{occ}(0.18,r_H)+17.44\}} \quad (19)$$

This equation slightly improves the good results of the original MOOH method, and yields significantly better results than the Atkinson method (see Table 2). Summation over all aldehydic H sites in the molecule corresponds to the third term of eq 1.

OH Addition to C=C Bonds. The OH addition to C=C bonds is the dominating degradation mechanism for olefinic compounds.[24,25] The respective reaction rates range from about 2×10^{-13} cm^3 $molecule^{-1}$ s^{-1} for tetrachloroethene to about 3 $\times 10^{-10}$ cm^3 $molecule^{-1}$ s^{-1} for some polyenes. The reaction sites are the sp^2 carbon atoms (see eq 9). Their individual reactivity with respect to OH addition is described by a function of their MOOH parameters. Here, hydrogen abstraction from sp^3 carbon atoms is of minor importance but was taken into account. Following the original MOOH method, we used the charge-limited π donor energy at sp^2 carbon with $q_\pi = 0.58$, $EQ^{\pi}_{occ}(0.58,r_C)$, and the energy-limited acceptor excess charge with a penetration energy ε of 2.8 eV, $QE_{vac}(2.8,r_C)$ to describe the rate constant of an individual sp^2 carbon atom. The original MOOH method was developed using the experimental rate constants of 58 olefinic compounds. We recalibrated it using a data set of 124 alkenes and derived the equation

$$k^{C=C}_{add}(r_C) = \exp\{1.52 \cdot EQ^{\pi}_{occ}(0.58,r_C) - 1.25 \cdot QE_{vac}(2.8,r_C) + 18.92\} \quad (20)$$

Application of eq 20 to all sp^2 carbons of a molecule that belong to double bonds leads to the fourth term of eq 1 for predicting log k_{OH}. Using this expression, we could improve the already good performance of the original parametrization for alkenes and achieved significantly better results than the Atkinson method (q^2 values of 0.88, 0.80 and 0.51, and *rms* values of 0.27, 0.28 and 0.55, respectively; see Table 2).

TABLE 2: Statistical Performance of the Re-Calibrated AM1-MOOH Method, of Its Original Klamt Parameterization, and of the Atkinson Increment Scheme[a]

Data set	Method	*n*	r^2	q^2	*rms*	*bias*	*me*	*mne*	*mpe*
mechanistic	AM1-MOOH	805	0.94	0.94	0.32	−0.01	0.23	−1.28	1.34
domain	Klamt	805	0.93	0.93	0.35	−0.06	0.25	−1.28	1.34
	Atkinson	805	0.93	0.92	0.35	0	0.2	−2.56	2.2
training set	AM1-MOOH	675	0.95	0.95	0.29	0	0.21	−1.03	1.08
	Klamt	675	0.94	0.93	0.33	−0.05	0.24	−1.28	1.11
	Atkinson	675	0.92	0.92	0.37	0	0.21	−2.56	2.2
test set	AM1-MOOH	130	0.87	0.86	0.43	−0.09	0.33	−1.28	1.34
(extrapolation)	Klamt	130	0.87	0.85	0.45	−0.11	0.34	−1.24	1.34
	Atkinson	130	0.95	0.95	0.26	−0.02	0.19	−0.49	1.02
saturated	AM1-MOOH	233	0.96	0.96	0.28	0	0.21	−1.02	1.02
hydrocarbons	Klamt	233	0.96	0.96	0.3	−0.02	0.23	−1.09	1.07
and ethers	Atkinson	233	0.93	0.93	0.39	0.01	0.24	−1.72	1.27
hydrogen bond	AM1-MOOH	148	0.79	0.78	0.37	−0.01	0.29	−1.03	1.08
acceptors	Klamt	148	0.76	0.7	0.43	−0.19	0.33	−1.22	0.91
(no aldehydes)	Atkinson	148	0.85	0.84	0.31	0.03	0.19	−0.87	1.61
ketones	AM1-MOOH	28	0.81	0.8	0.32	0.07	0.25	−1.03	0.36
	Klamt	28	0.81	0.8	0.31	−0.07	0.2	−1.16	0.24
	Atkinson	28	0.89	0.89	0.23	−0.01	0.15	−0.8	0.38
esters	AM1-MOOH	38	0.87	0.87	0.27	−0.01	0.19	−0.77	0.59
(no formyl esters)	Klamt	38	0.89	0.79	0.34	−0.23	0.28	−0.94	0.41
	Atkinson	38	0.88	0.88	0.26	−0.03	0.18	−0.64	0.93
alcohols	AM1-MOOH	55	0.77	0.77	0.41	0.02	0.33	−0.98	1.08
	Klamt	55	0.76	0.67	0.49	−0.2	0.39	−1.22	0.91
	Atkinson	55	0.86	0.79	0.39	0.11	0.22	−0.37	1.61
acids	AM1-MOOH	6	0.71	0.66	0.27	−0.07	0.22	−0.42	0.3
	Klamt	6	0.66	0.46	0.35	0.16	0.2	−0.11	0.73
	Atkinson	6	0.76	0.65	0.28	0.12	0.16	−0.1	0.6
aldehydes	AM1-MOOH	29	0.9	0.89	0.27	0.02	0.21	−0.48	0.79
	Klamt	29	0.9	0.88	0.28	0.06	0.19	−0.35	1.11
	Atkinson	29	0.65	0.57	0.55	0.22	0.32	−0.32	2.2
alkenes	AM1-MOOH	124	0.88	0.88	0.24	0.01	0.16	−0.67	0.99
	Klamt	124	0.85	0.8	0.3	−0.02	0.18	−1.28	0.86
	Atkinson	124	0.62	0.51	0.48	−0.05	0.23	−2.56	1.29
aromatics	AM1-MOOH	134	0.9	0.9	0.27	0.01	0.19	−0.89	0.9
	Klamt	134	0.89	0.88	0.29	−0.03	0.22	−1.06	0.95
	Atkinson	134	0.94	0.94	0.21	−0.02	0.14	−0.65	0.83
alkynes	AM1-MOOH	7	0.95	0.94	0.12	0.03	0.09	−0.16	0.18
	Klamt	7	0.97	0.96	0.1	0.04	0.08	−0.14	0.13
	Atkinson	7	0.99	0.99	0.06	−0.01	0.04	−0.08	0.08

[a] The total set contains 805 compounds, of which 675 compounds were used as training set for AM1-MOOH. *n* = number of compounds; q^2 = predictive squared correlation coefficient (eq 2); *rms* = root-mean-square error; *bias* = systematic error; *me* = mean error; *mne* = maximum negative error (largest underestimation); *mpe* = maximum positive error (largest overestimation).

For *cis*-1,3,5-hexatriene, a rate constant of 1.1×10^{-13} cm^3 molecule^{-1} s^{-1} has been reported.[36] This value is indeed small compared to similar compounds. Interestingly, both AM1-MOOH and the Atkinson method overestimate this k_{OH} value by more than 3 log units (3.08 and 3.01, respectively), and a similar overestimation is achieved by the original Klamt parametrization (3.16). At the same time, the overall intercorrelation of the AM1-MOOH and Atkinson prediction errors is very low ($r^2 = 0.10$), reflecting the fundamental difference in methodology of the two models. Thus, the high agreement in prediction error for *cis*-1,3,5-hextatriene between the two otherwise quite different methods suggests that its experimental value either reflects an unusual mechanism different from the other alkenes, or is doubtful. Accordingly, we suggest to redetermine k_{OH} for this compound, expecting a value in the range of 1.2×10^{-10} cm^3 molecule^{-1} s^{-1}.

OH Addition to Aromatic Rings. Most aromatic compounds are degraded by addition of OH radicals to aromatic carbon (eq 8).[24,25] Again, hydrogen abstraction from alkyl substituent groups plays a minor role that is nevertheless taken into consideration. Using 134 aromatic compounds, we recalibrated the MOOH model equation for OH addition to aromatic rings. In contrast to the original parametrization, heteroaromatic compounds and condensed aromatics were included in the calibration. The experimental rate constants range from about 3×10^{-14} cm^3 molecule^{-1} s^{-1} for hexachlorobenzene to about 5.5×10^{-10} cm^3 molecule^{-1} s^{-1} for 1-naphthol. As before,[4] the readiness of aromatic carbon for OH addition was quantified through the effective donor energy with $E_{ref} = 2.23$ eV, $EE_{occ}(2.23,r_C)$, and the substituent deformation energy, Δ^{aro}_{def}. Recalibration resulted in the following equation:

$$k^{aro}_{add}(r_C) = \exp\left\{\frac{8.15}{(1+\exp\{-3.45\cdot(EE_{occ}(2.23,r_C)+10.55)\})} - 0.127\cdot\Delta^{aro}_{def} - 3.23\right\} \quad (21)$$

Although the resultant statistics are slightly superior to the original parametrization, the Atkinson method still performs best for this subset of compounds (*rms* values of 0.27, 0.29 and 0.21, respectively; see Table 2).

Although data for nitro-aromatics and aryl isothiocyanates are available,[36−38] these compounds were left out of the present calibration due to significant deviations between predicted and measured rate constants. Accordingly, these compounds do not belong to the chemical domain of eq 21. The error for nitro-aromatics seems to correlate with the experimental rate constant: The smallest compound is slightly overestimated, whereas for the remaining compounds, underestimation increases with increasing experimental rate constant ($r^2 = 0.83$). Nonetheless, the observed errors for nitro-aromatics do not exceed 1 log unit except for 5-methyl-2-nitrophenol predicted with a log k_{OH} error of 1.22.

Aryl isothiocyanates are systematically underestimated by both the Atkinson and the MOOH approach. Note, however, that the currently determined mean error of −1.09 for aryl isothiocyanates could be considered and corrected for when tentatively exploring the k_{OH} range of aryl isothiocyanates through application of eq 21. The prediction errors for nitro-aromatics and aryl isothiocyanates are assumed to originate from additional or modified reaction pathways involving the respective functional groups. These aspects may be addressed by a respective extension of the approach in future work.

OH Addition to C≡C Bonds. The original MOOH method was developed using a data set of only 6 alkynes. Since then, the experimental rate constant of only one further alkyne has been published. For the calibration, hydrogen abstraction from aliphatic carbon has to be taken into account when summing up all contributions to k_{OH} (see eq 1). The resultant regression equation to model OH addition to triple bonds (eq 10) is

$$k^{C\equiv C}_{add}(r_C) = \exp\{2.37\cdot EQ_{occ}(0.58,r_C) + 26.19\} \quad (22)$$

Interestingly, use of the recalibrated equation for $k^{C}_{H\text{-}abs}$ led to slightly inferior statistics for $k^{C\equiv C}_{add}$ than when employing the original parametrization, although the difference is only marginal (*rms* 0.12 vs 0.10) and refers to only seven alkynes. Note further that the recalibrated equation for H abstraction from sp^3 carbon yields better results for a much larger compound set (*rms* 0.28 vs 0.30 for 233 compounds; see Table 2). For the sake of consistency we therefore prefer to account for $k^{C}_{H\text{-}abs}$ in alkynes through eq 22 rather than through the original regression equation.

Multifunctional Compounds. As mentioned above, some groups of compounds with mixed functional groups were excluded from calibration to avoid cross-contamination of pathway-specific model parameters. Note that for multifunctional compounds, k_{OH} is determined by the concurrent presence of several fast degradation pathways in addition to H abstraction from aliphatic carbon (if applicable). Based on this consideration, the following compound classes were left out of calibration: 12 formyl esters, 6 hydroxylated aldehydes, 3 keto-aldehydes, 2 hydroxylated alkynes, 29 aromatics with oxidated and/or olefinic side chains, and 64 oxidated alkenes. Moreover, initial analysis revealed a poor model performance for halomethanes, and accordingly this subset of 14 compounds was also removed from the training set. The latter thus consisted of 675 compounds, all of which react by direct hydrogen abstraction from aliphatic carbon and up to one additional degradation mechanism, except for aldehydes, with the CHO group introducing two additional mechanisms ($k^{CHO}_{H\text{-}abs}$ and $k^{C(O)}_{H\text{-}abs}$, see eqs 6 and 7).

The remaining 130 compounds could be treated as test set, keeping in mind that these mostly bi- and multifunctional compounds do not reflect the chemical composition of the training set and thus would be considered to be outside the chemical domain of the current (and previous) MOOH model. However, this data set may be used to test whether the model is able to predict experimental rate constants, and whether it is possible to extrapolate from mono- to bi- and multifunctional compounds.

As can be seen from Table 2, tentative application of AM1-MOOH to this subset yields indeed good results ($q^2 = 0.86$, $rms = 0.43$). Here, the Atkinson increment scheme shows the best performance ($q^2 = 0.95$, $rms = 0.26$), keeping in mind that some of these compounds had been used for the respective fitting procedure.[1,3] For future extensions of the MOOH method to these and other multifunctional compounds, attention should be paid to differentiating between model errors due to the underlying semiempirical wave function, and model errors due to reaction pathways not yet considered and thus not yet encoded in respective local reactivity parameters.

Conclusions

The current study demonstrates the scope of the MOOH approach to predict rate constants of organic compounds for indirect photolysis through reaction with OH radicals, k_{OH}, from molecular structure. It can be easily applied by the combined use of the MOPAC package and the MOOH software. For the total set of 805 compounds, the model performance is superior to the prominent Aktinson increment scheme and thus provides a valuable alternative employing a totally different methodology.

In the context of REACH as well as when screening—possibly not yet synthesized—chemical structures for their atmospheric lifetime, both AM1-MOOH and the Atkinson scheme could be used as components of a consensus modeling approach. With the latter, confidence in model predictions is increased through agreement between predictions of methodologically different models. Correspondingly, substantial disagreement in model predictions indicates cases of less confidence and an accordingly larger error margin than expected from conventional performance statistics, considering also the class-specific model performances as described in the present study. As was demonstrated with *cis*-1,3,5-hexatriene, large prediction errors from both models can be taken as hint to reconsider either the mechanistic pathway governing k_{OH} or the quality of its experimental value. Future extensions of the MOOH approach should pay attention to shortcomings possibly imposed by the presently underlying semiempirical wave function (AM1-MOOH), to addressing multifunctional compounds explicitly, and to consider degradation pathways associated with other heteroatoms such as sulfur and nitrogen.

Acknowledgment. We thank Dr. Andreas Klamt for making available the original MOOH source code. This research was financially supported by the European Commission through the projects NOMIRACLE (FP6 Contract No. 003956) and OSIRIS (Contract No. 037017).

Supporting Information Available: Data set of experimental OH radical reaction rate constants for 805 compounds. This material is available free of charge via the Internet at http://pubs.acs.org. A licensed copy of an executable program to automatically predict the rate constant of indirect photolysis through reaction with OH radicals, k_{OH}, from MOPAC output files can be obtained upon request from the corresponding author.

References and Notes

(1) Atkinson, R. Kinetics and mechanisms of the gas-phase reactions of the hydroxyl radical with organic compounds under atmospheric conditions. *Chem. Rev.* **1985**, *85*, 69–201.

(2) Atkinson, R. A structure-activity relationship for the estimation of rate constants for the gas-phase reactions of OH radicals with organic compounds. *Int. J. Chem. Kinet.* **1987**, *19*, 799–828.

(3) Kwok, E. S. C.; Atkinson, R. Estimation of Hydroxyl Radical Reaction-Rate Constants for Gas-Phase Organic-Compounds Using A Structure-Reactivity Relationship - An Update. *Atmos. Environ.* **1995**, *29*, 1685–1695.

(4) Klamt, A. Estimation of gas-phase hydroxyl radical rate constants of organic compounds from molecular orbital calculations. *Chemosphere* **1993**, *26*, 1273–1289.

(5) Klamt, A. Estimation of gas-phase hydroxyl radical rate constants of oxygenated compounds based on molecular orbital calculations. *Chemosphere* **1996**, *32*, 717–726.

(6) Sabljic, A.; Peijnenburg, W. Modeling lifetime and degradability of organic compounds in air, soil, and water systems. *Pure Appl. Chem.* **2001**, *73*, 1331–1348.

(7) Meylan, W. M.; Howard, P. H. A review of quantitative structure-activity relationship methods for the prediction of atmospheric oxidation of organic chemicals. *Environ. Toxicol. Chem.* **2003**, *22*, 1724–1732.

(8) Schüürmann, G.; Ebert, R.-U.; Nendza, M.; Dearden, J. C.; Paschke, A.; Kühne, R. Predicting fate-related physicochemical properties. In *Risk assessment of chemicals: An Introduction*, 2nd ed.; van Leeuwen, C. J., Vermeire, T. G., Eds.; Springer: Dordrecth, The Netherlands, 2007; pp 375−426.

(9) *AOPWIN. Atmospheric oxidation program for MS-Windows*; U.S. Environmental Protection Agency: Washington, DC, 2000.

(10) Meylan, W. M.; Howard, P. H. Computer estimation of the Atmospheric gas-phase reaction rate of organic compounds with hydroxyl radicals and ozone. *Chemosphere* **1993**, *26*, 2293–2299.

(11) Dewar, M. J. S.; Zoebisch, E. G.; Healy, E. F.; Stewart, J. J. P. AM1: A New General Purpose Quantum Mechanical Molecular Model. *J. Am. Chem. Soc.* **1985**, *107*, 3902–3909.

(12) *MOPAC 93,* Revision 2, Fujitsu Limited, 9-3, Nakase 1-Chome, Mihama-ku, Chiba-city, Chiba 261, Japan, and Stewart Computational Chemistry, 15210 Paddington Circle, Colorado Springs, CO, 1994.

(13) Schüürmann, G.; Kühne, R.; Kleint, F.; Ebert, R.-U.; Rothenbacher, C.; Herth, P. A software system for automatic chemical property estimation from molecular structure. In *QSAR in Environmental Sciences*; Chen, F., Schüürmann, G., Eds.; SETAC Press: Pensacola, FL, 1997; pp 93−114.

(14) Becke, A. D. Density-functional thermochemistry. III. The role of exact exchange. *J. Chem. Phys.* **1993**, *98*, 5648–5652.

(15) Clark, T.; Chandrasekhar, J.; Spitznagel, G. W.; Schleyer, P. v. R. Efficient diffuse function-augmented basis sets for anion calculations. III. The 3-21+G basis set for first-row elements, Li-F. *J. Comput. Chem.* **1983**, *4*, 294–301.

(16) Frisch, M. J.; Pople, J. A.; Binkley, J. S. Self-consistent molecular orbital methods 25. Supplementary functions for Gaussian basis sets. *J. Chem. Phys.* **1984**, *80*, 3265–3269.

(17) Francl, M. M.; Pietro, W. J.; Hehre, W. J.; Binkley, J. S.; Gordon, M. S.; DeFrees, D. J.; Pople, J. A. Self-Consistent Molecular Orbital Methods. XXIII. A polarization-type basis set for second-row elements. *J. Chem. Phys.* **1982**, *77*, 3654–3665.

(18) Lee, C.; Yang, W.; Parr, R. G. Development of the Colle-Salvetti correlation-energy formula into a functional of the electron density. *Phys. Rev. B* **1988**, *37*, 785–789.

(19) Hehre, W. J.; Ditchfield, R.; Pople, J. A. Self-Consistent Molecular Orbital Methods. XII. Further Extensions of Gaussian-Type Basis Sets for Use in Molecular Orbital Studies of Organic Molecules. *J. Chem. Phys.* **1972**, *56*, 2257–2261.

(20) Frisch, M. J.; Trucks, G. W.; Schlegel, H. B.; Scuseria, G. E.; Robb, M. A.; Cheeseman, J. R.; Montgomery, J. A.; Vreven, T.; Kudin, K. N.; Burant, J. C.; Millam, J. M.; Iyengar, S. S.; Tomasi, J.; Barone, V.; Mennucci, B.; Cossi, M.; Scalmani, G.; Rega, N.; Petersson, G. A.; Nakatsuji, H.; Hada, M.; Ehara, M.; Toyota, K.; Fukuda, R.; Hasegawa, J.; Ishida, M.; Nakajima, T.; Honda, Y.; Kitao, O.; Nakai, H.; Klene, M.; Li, X.; Knox, J. E.; Hratchian, H. P.; Cross, J. B.; Adamo, C.; Jaramillo, J.; Gomperts, R.; Stratmann, R. E.; Yazyev, O.; Austin, A. J.; Cammi, R.; Pompelli, C.; Ochterski, J. W.; Ayala, P. Y.; Morokuma, Keiji; Voth, G. A.; Salvador, P.; Dannenberg, J. J.; Zakrzewski, V. G.; Dapprich, S.; Daniels, A. D.; Strain, M. C.; Farkas, O.; Malick, D. K.; Rabuck, A. D.; Raghavavachari, K.; Foresman, J. B.; Ortiz, J. V.; Cui, Q.; Baboul, A. G.; Clifford, S.; Cioslowski, J.; Stefanov, B. B.; Liu, G.; Liashenko, A.; Piskorz, P.; Komaromi, I.; Martin, R. L.; Fox, D. J.; Keith, T.; Al-Laham, M. A.; Peng, C. Y.; Nanayakkara, A.; Challacombe, M.; Gill, P. M. W.; Johnson, B.; Chen, W.; Wong, M. W.; Gonzalez, C.; Pople, J. A. *Gaussian 03, Revision C.02*; Gaussian, Inc.: Pittsburgh, PA, 2003.

(21) Marquardt, D. W. An algorithm for least-squares estimation of nonlinear parameters. *SIAM J. Appl. Math* **1963**, *11*, 431–441.

(22) Brandt, S. *Datenanalyse*, 4 ed.; Spektrum Akademischer Verlag: Heidelberg/Berlin, Germany, 1999.

(23) Kühne, R.; Ebert, R.-U.; Schüürmann, G. Prediction of the temperature dependency of Henry's Law constant from chemical structure. *Environ. Sci. Technol.* **2005**, *39*, 6705–6711.

(24) Seinfeld, J. H.; Pandis, S. N. *Atmospheric Chemistry and Physics: From Air Pollution to Climate Change*; J. Wiley: New York, 1998.

(25) Atkinson, R.; Arey, J. Atmospheric degradation of volatile organic compounds. *Chem. Rev.* **2003**, *103*, 4605–4638.

(26) Smith, I.; Ravishankara, A. R. Role of Hydrogen-Bonded Intermediates in the Bimolecular Reactions of the Hydroxyl Radical. *J. Phys. Chem. A* **2002**, *106*, 4798–4807.

(27) Mellouki, A.; Le Bras, G.; Sidebottom, H. Kinetics and Mechanisms of the Oxidation of Oxygenated Organic Compounds in the Gas Phase. *Chem. Rev.* **2003**, *103*, 5077–5096.

(28) Aloisio, S.; Francisco, J. S. Complexes of Hydroxyl and Hydroperoxyl Radical with Formaldehyde, Acetaldehyde, and Acetone. *J. Phys. Chem. A* **2000**, *104*, 3211–3224.

(29) D'Anna, B.; Bakken, V.; Beukes, J. A.; Nielsen, C. J.; Brudnik, K.; Jodkowski, J. T. Experimental and theoretical studies of gas phase NO_3 and OH radical reactions with formaldehyde, acetaldehyde and their isotopomers. *Phys. Chem. Chem. Phys.* **2003**, *5*, 1790–1805.

(30) Galano, A.; Alvarez-Idaboy, J. R.; Bravo-Perez, G.; Ruiz-Santoyo, M. E. Gas phase reactions of C-1-C-4 alcohols with the OH radical: A quantum mechanical approach. *Phys. Chem. Chem. Phys.* **2002**, *4*, 4648–4662.

(31) Galano, A.; Alvarez-Idaboy, J. R.; Ruiz-Santoyo, M. E.; Vivier-Bunge, A. Rate coefficient and mechanism of the gas phase OH hydrogen abstraction reaction from formic acid: A quantum mechanical approach. *J. Phys. Chem. A* **2002**, *106*, 9520–9528.

(32) Rosado-Reyes, C. M.; Francisco, J. S. Atmospheric oxidation pathways of acetic acid. *J. Phys. Chem. A* **2006**, *110*, 4419–4433.

(33) Vandenberk, S.; Vereecken, L.; Peeters, J. The acetic acid forming channel in the acetone + OH reaction: A combined experimental and theoretical investigation. *Phys. Chem. Chem. Phys.* **2002**, *4*, 461–466.

(34) Vasvári, G.; Szilágyi, I.; Bencsura, Á.; Dóbé, S.; Bérces, T.; Henon, E.; Canneaux, S.; Bohr, F. Reaction and complex formation between OH radical and acetone. *Phys. Chem. Chem. Phys.* **2001**, *3*, 551–555.

(35) Schüürmann, G. Quantum Chemical Descriptors in Structure-Activity Relationships — Calculation, Interpretation, and Comparison of Methods. In *Predicting Chemical Toxicity and Fate*; Cronin, M. T. D., Livingstone, D. J., Eds.; CRC Press: Boca Raton, FL, 2004; pp 85—149.

(36) Beauman, J. A.; Howard, P. H. *Physprop database*; Syracuse Research Corporation: Syracuse, NY, 2001.

(37) Bejan, I.; Barnes, I.; Olariu, R.; Zhou, S.; Wiesen, P.; Benter, T. Investigations on the gas-phase photolysis and OH radical kinetics of methyl-2-nitrophenols. *Phys. Chem. Chem. Phys.* **2007**, *9*, 5686–5692.

(38) Sommerlade, R.; Ekici, P.; Parlar, H. Gas phase reaction of selected isothiocyanates with OH radicals using a smog chamber-mass analyzer system. *Atmos. Environ.* **2006**, *40*, 3306–3315.

JP8052218